

## Supporting Information

### Multifunctional Anthraquinone-Sulfonic Potassium Salts Passivates the Buried Interface for Efficient and Stable Planar Perovskite Solar Cells

Yanqiang Hu<sup>a,b</sup>, Zong Xu<sup>a</sup>, Zhi Wang<sup>a</sup>, Yifan Zhou<sup>a</sup>, Wenwu Song<sup>a</sup>, Yushuang Gao<sup>b</sup>, Guangping Sun<sup>a</sup>, Tongming Sun<sup>a</sup>, Shufang Zhang<sup>b,\*</sup>, Yanfeng Tang<sup>a,\*</sup>

<sup>a</sup>College of Chemistry and Chemical Engineer, Nantong University, Nantong 226001, Jiangsu, China.

<sup>b</sup>School of Physics and Photoelectric Engineering, Ludong University, Yantai 264025, Shandong, China.

This file includes **Figure S1-S12** and **Table S1-S3**:

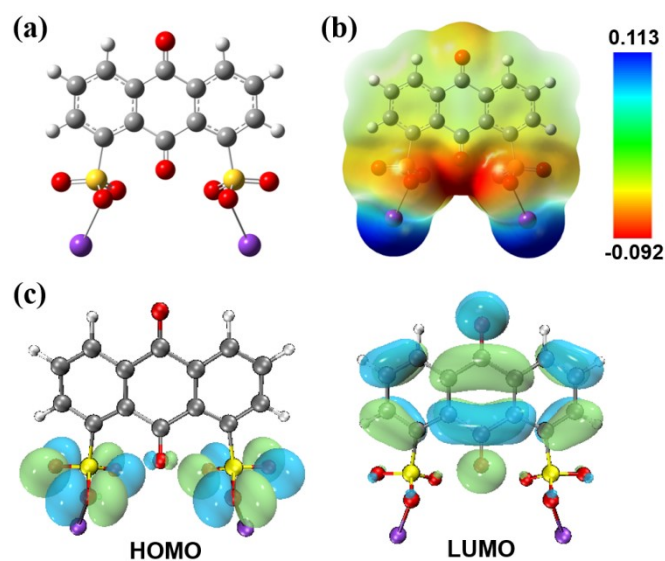


**Figure S1.** (a) Molecular structure, (b) electrostatic surface potential map, and (c) calculated frontier molecular orbitals of ASPS molecule.

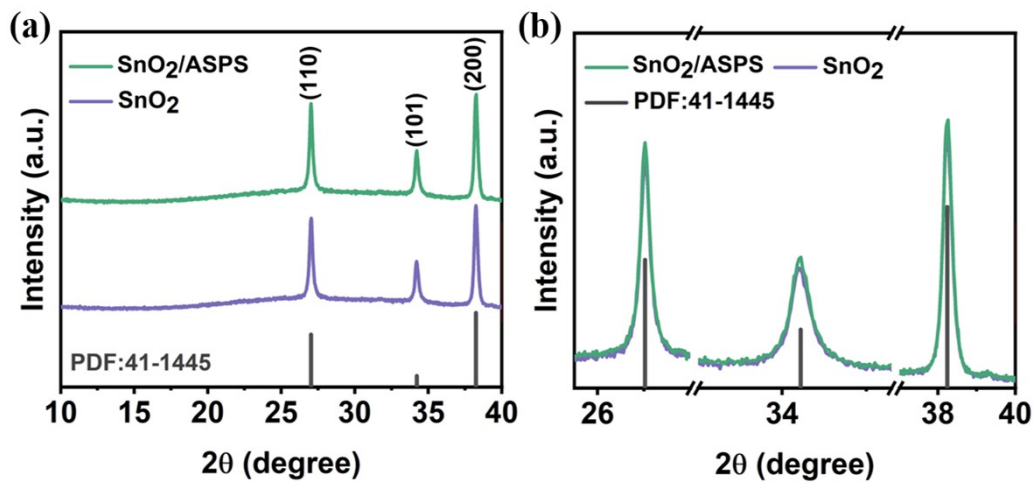


Figure S2. XRD patterns of SnO<sub>2</sub> film without and with ASPS modification.

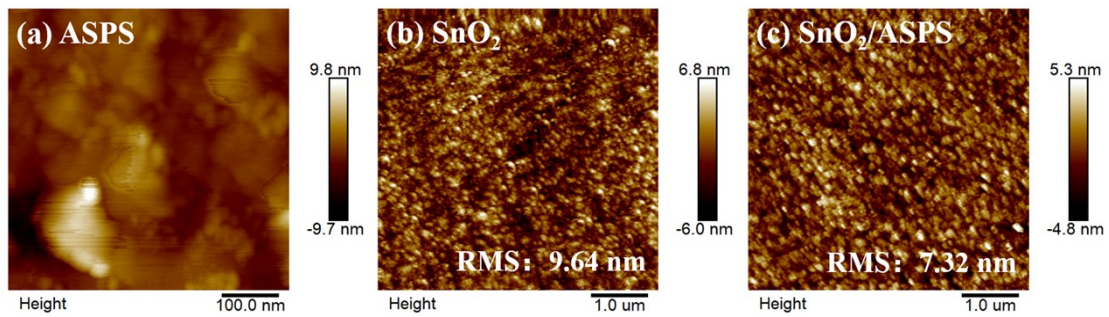


Figure S3. AFM images of (a) ASPS, (b) SnO<sub>2</sub> and (c) ASPS-modified SnO<sub>2</sub> on glass substrates, respectively.

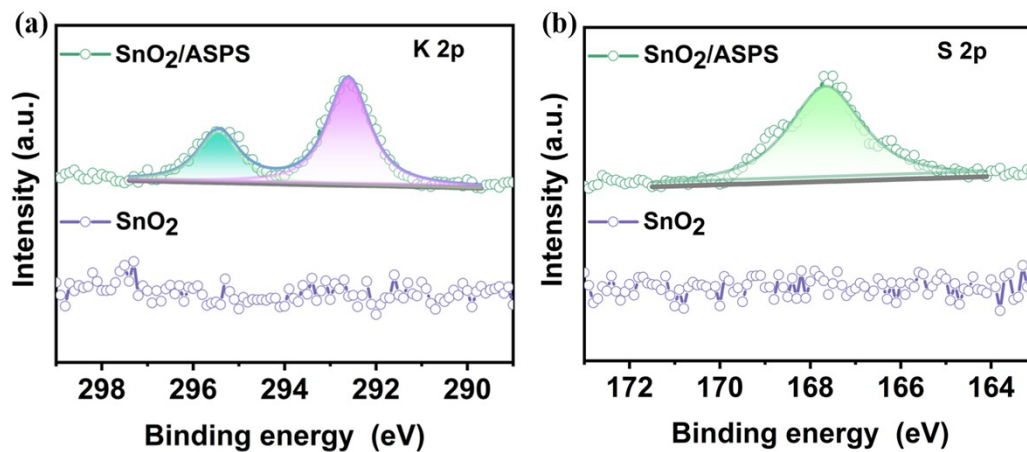
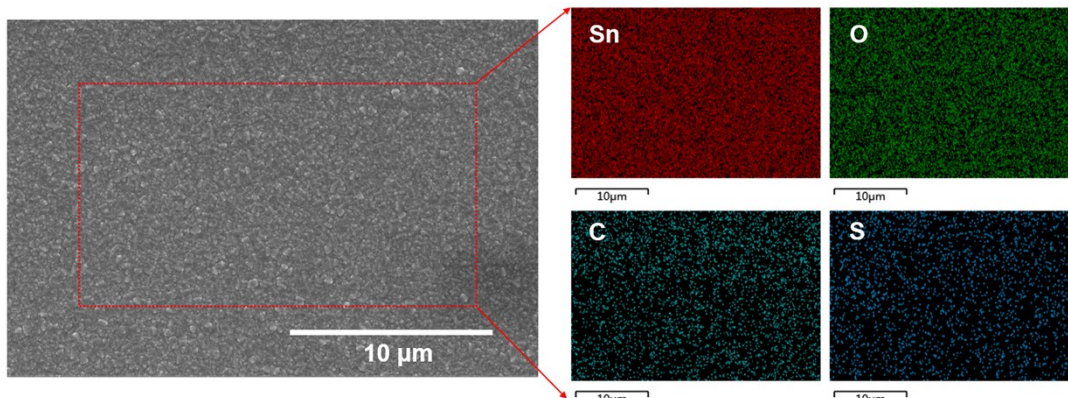
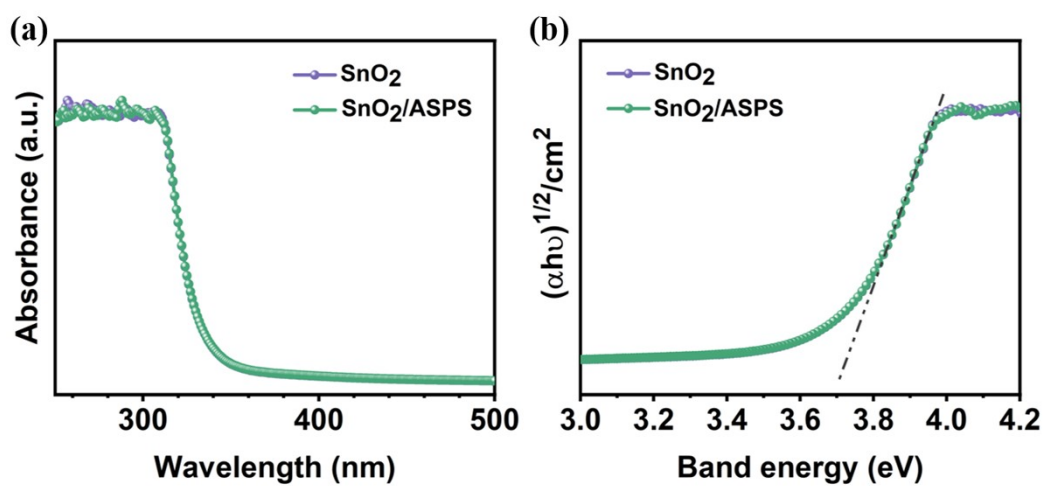


Figure S4. (a) K 2p, and (c) S 2p XPS spectra of SnO<sub>2</sub> and SnO<sub>2</sub>/ASPS substrates, respectively.



**Figure S5.** Top-view SEM and corresponding energy dispersive spectroscopy (EDS) mapping of SnO<sub>2</sub>/ASPS substrate, respectively.



**Figure S6.** (a) Optical absorbance and (d) corresponding Tauc plots of SnO<sub>2</sub> film without or with ASPS modification.

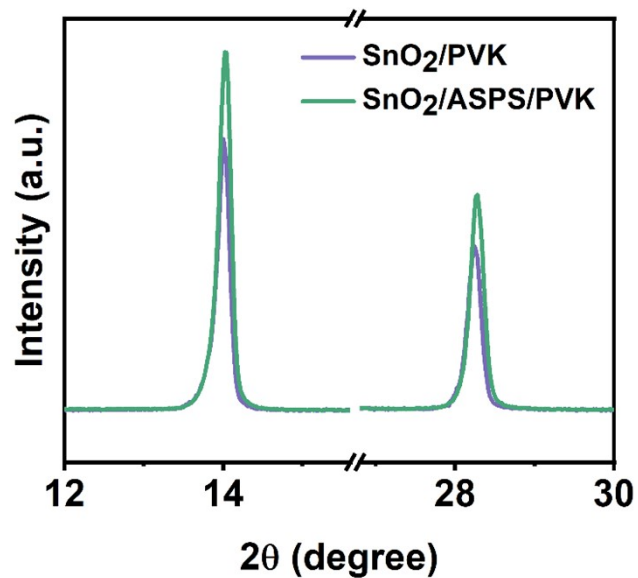


**Figure S7.** Region amplified XRD pattern of PVK films deposited on SnO<sub>2</sub> and SnO<sub>2</sub>/ASPS substrates.

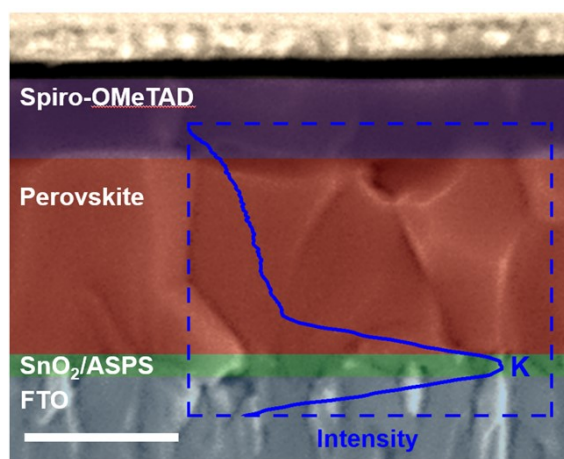


**Figure S8.** Elemental scanning in a liner mode through the cross-section of SnO<sub>2</sub>/ASPS/PVK. Scale bar: 500 nm.

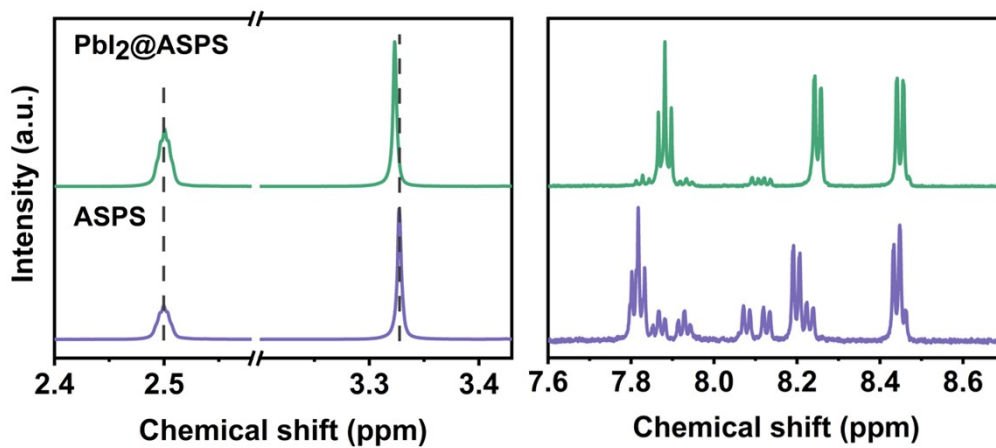


**Figure S9.** Liquid-state  $^1\text{H}$  NMR spectra of pure ASPS and  $\text{Pbl}_2@ASPS$  dissolving in  $\text{DMSO}-d_6$ , respectively.

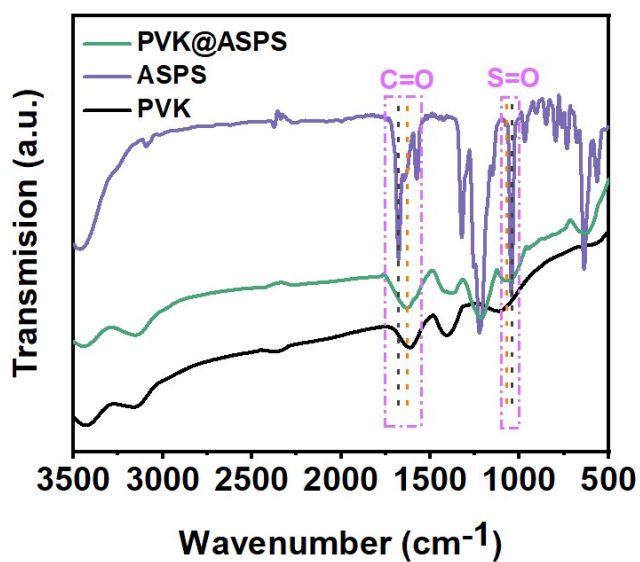


**Figure S10.** FTIR spectra of PVK, pure ASPS powder, and  $\text{PVK}@ASPS$ , respectively.

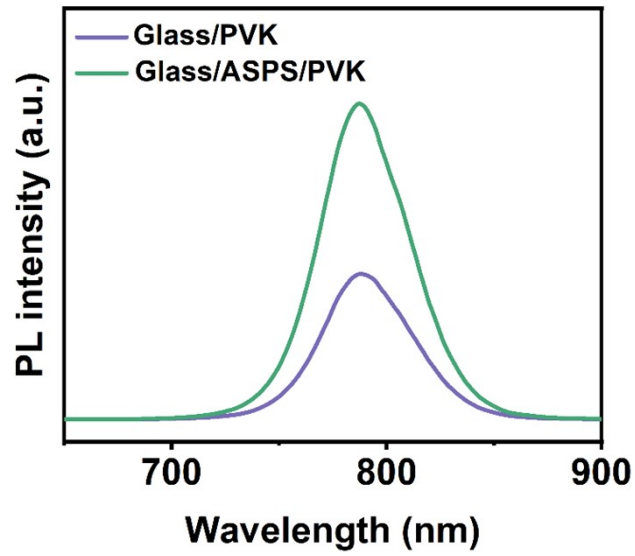


**Figure S11.** The steady-state PL spectra of PVK films deposited on SnO<sub>2</sub> and SnO<sub>2</sub>/ASPS substrates.

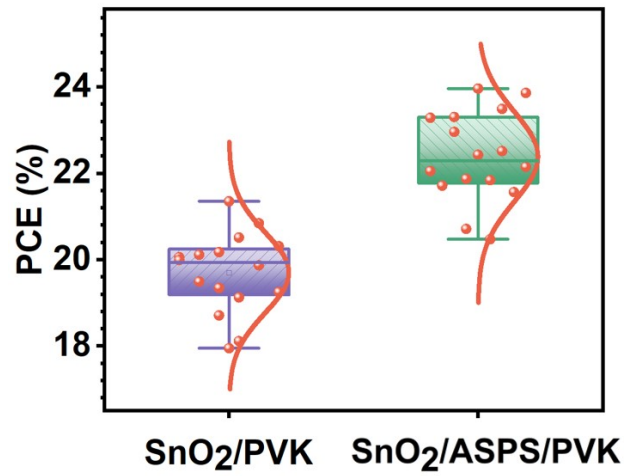


**Figure S12.** Statistical distribution of PCE of the controlled and optimized PSCs. The statistical data were collected from 16 cells for each case.

**Table S1.** The photovoltaic parameters of the champion devices with different concentrations of ASPS.

ASPS (mg/mL)	Voc (V)	Jsc (mA/cm <sup>2</sup> )	FF (%)	PCE (%)
0.0	1.10	24.47	79.37	21.36
0.25	1.13	24.51	80.83	22.39
0.5	1.16	24.57	81.98	23.36
0.75	1.17	24.76	82.70	23.96
1.0	1.15	24.43	79.83	22.43

**Table S2.** The photovoltaic parameters of the champion devices with AD, ADA, and ASPS, respectively.

Sample		Voc (V)	Jsc (mA/cm <sup>2</sup> )	FF (%)	PCE (%)
AD	FS	1.12	24.59	78.83	21.71
	RS	1.16	24.61	81.32	23.21
ADA	FS	1.13	24.67	80.03	22.31
	RS	1.16	24.70	82.86	23.74
ASPS	FS	1.16	24.75	80.16	23.01
	RS	1.17	24.76	82.70	23.96

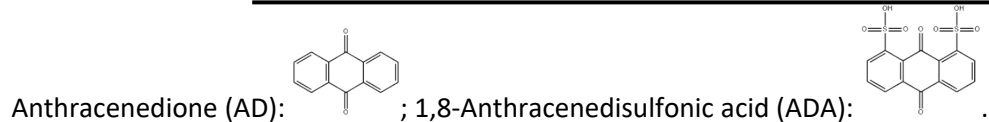


**Table S3.** Initial photovoltaic parameters of the stability test device under reverse scanning.

	Voc (V)	Jsc (mA/cm <sup>2</sup> )	FF (%)	PCE (%)	
Storage stability	0.0	1.09	24.45	78.56	20.94
	0.75	1.16	24.74	80.96	23.23
Thermal stability	0.0	1.08	24.46	78.43	20.72
	0.75	1.15	24.70	81.12	23.04

---

Light stability	0.0	1.08	24.45	78.34	20.69
	0.75	1.14	24.73	80.70	22.75

---